

Full length article

# Hole-injection barrier across the intermolecular interaction mediated interfacial DNTT layer

Subhankar Mandal, Saugata Roy, Md Saifuddin, Satyajit Hazra \*

Saha Institute of Nuclear Physics, A CI of Homi Bhabha National Institute, 1/AF Bidhannagar, Kolkata, 700064, India

## ARTICLE INFO

## Keywords:

Organic semiconductor  
Wetting–dewetting  
Interfacial layer  
 $\pi$ -orbital overlapping  
Intermolecular interaction  
Charge injection barrier

## ABSTRACT

The electronic structures and morphology of dinaphthothienothiophene (DNTT) thin films on highly oriented pyrolytic graphite (HOPG) and polycrystalline Au (pc-Au) substrates have been investigated using photoelectron spectroscopy and atomic force microscopy techniques to better correlate the charge-injection barrier with the interfacial structure. DNTT molecules follow Stranski–Krastanov-type growth mode, i.e., highly-dewetted islands/fibers above a relatively-wetted interfacial layer, on both the substrates, but distinctively different electronic structures. On the HOPG surface, the as-grown and thermal-annealed films show a broad and a sharp highest occupied molecular orbital (HOMO) bands, respectively. On the pc-Au surface, a significantly split HOMO band and a reduced hole-injection barrier are observed in a monolayer thick film, for the first time, which are absent in other thick films. Such splitting indicates a presence of a strong intermolecular interaction in the interfacial layer, presumably due to the frontier  $\pi$ -orbital overlapping arising from partially-covered densely-packed herringbone-like arranged molecules. The dewetted-fibers seem to form with up-right oriented molecules having negligible interaction, which desorb easily by thermal annealing to retain the highly-stable interfacial layer. The reduction of the hole-injection barrier at the DNTT/pc-Au interface, due to the formation of such interfacial layer having strong intermolecular interaction, has an immense importance in increasing the charge-injection efficiency from a practical electrode.

## 1. Introduction

In recent years, a rapid progress of organic semiconductor (OSC) based devices [1], such as organic light-emitting diode (OLED) [2, 3], organic photovoltaic (OPV) [4,5], and organic thin-film transistor (OTFT) [6–9] has been observed. The unique properties, namely light weight, low-cost production, low-temperature processing, mechanical flexibility, and abundant availability, of OSCs compared to their conventional inorganic counterparts make them attractive. However, lack of air and thermal stability is one of the key concern with most of them, where much weaker (van der Waals type noncovalent) interactions are usually present compared to the strong (covalent) interactions in the inorganic materials [10]. Recently, some OSCs have been developed to overcome that concern and dinaphtho[2,3-b:20,30-f]thieno[3,2-b]thiophene (DNTT,  $C_{22}H_{12}S_2$ ) is one of them [11]. It is basically a highly  $\pi$ -extended heteroarene having six fused aromatic rings, where the two fused thiophene rings are at center and two fused benzene rings are at both ends (as shown in Fig. S1 of the Supporting Information). Such DNTT has lower HOMO (highest occupied molecular orbital) level, wider HOMO-LUMO (lowest unoccupied molecular orbital) gap (obtained from molecular orbital calculation) and higher

ionization potential (IP = 5.44 eV, as estimated by ultraviolet photoelectron spectroscopy and reproduced by density functional theory calculation) [12] compared to those of pentacene (IP = 4.85 eV) [13], which are known to be responsible for its higher air stability.

DNTT molecule, apart from having good air and thermal stability [9, 12,14], is known to demonstrate excellent charge carrier mobility [11, 15–17]. A strong intermolecular interaction was found to present in this molecule, which has a real impact on its charge transport properties [18]. An effective overlapping of its molecular orbitals was also found sometimes, which makes the molecule more promising for the potential application as a high-performance organic field-effect transistor [18,19]. The orientation, packing and coverage of the molecules in the film, especially near the film–substrate interface, are important for its promising properties [20–24]. The presence of flat-lying interfacial layer beneath the up-right oriented molecular film on  $SiO_2/Si$  substrate was proposed by Jung et al. [25] whereas only an up-right oriented molecular structure on  $SiO_2$  substrate was proposed by Breuer et al. [26]. Dielectric roughness dependence morphology and charge transport property of DNTT was recently studied by Geiger et al. [27]. Further, distinct molecular orientations on single crystalline (sc) and

\* Corresponding author.

E-mail address: [satyajit.hazra@saha.ac.in](mailto:satyajit.hazra@saha.ac.in) (S. Hazra).

polycrystalline (pc) noble metallic surfaces were revealed from the study of interfacial and film structures [28,29]. A splitting of HOMO level of 0.5 eV was observed in the densely-packed monolayer of DNTT on sc-Au(111) and not in the loosely-packed monolayer [19]. Such splitting was attributed to the effective overlapping of DNTT molecular orbitals in the presence of a strong intermolecular interaction in the densely-packed monolayer on the sc-Au(111). The splitting of HOMO level of the semiconducting material due to molecular orbital overlapping can be crucial to the efficiency of the charge-carrier injection to and extraction from the electrode. However, for that, the presence of such effect on a pc-metal, which can act as a practical electrode, is important. Unfortunately, not much attempts have been made so far, to verify the presence of any HOMO level splitting due to the interfacial DNTT layer on the pc-metal surface by correlating the interfacial electronic structure (i.e., the molecular interaction) with its molecular structure (namely wetting, coverage, orientation and packing).

In the present work, we have studied the electronic structures of the DNTT thin films on pc-Au and highly oriented pyrolytic graphite (HOPG) surfaces and their evolution with the film thickness and thermal annealing (AN) using in-situ ultraviolet and X-ray photoelectron spectroscopic (UPS and XPS) techniques to predict the molecular organization and/or packing near the film/substrate interface. Atomic force microscopy (AFM) technique was also used to substantiate the electronic structure of the interface with the molecular structure of DNTT. Indeed, the electronic structure of the DNTT film on the pc-Au surface is found distinctively different from that on the HOPG surface, suggesting different molecular organization on two different surfaces. In fact, a splitting of the HOMO level in the DNTT film, at the monolayer region, on the pc-Au surface is observed for the first time that was earlier observed on the sc-Au(111) surface due to the presence of densely-packed phase of the molecules at the interface [19]. The XPS results ruled out the presence of any strong substrate–molecule interaction at the DNTT/Au interface, suggesting the observed splitting of the HOMO level is due to the formation of densely-packed herringbone-like monolayer phase. The XPS and AFM results, before and after thermal annealing, further substantiate the formation of such interfacial phase having extra-stability. However, such densely-packed interfacial phase (or HOMO level splitting) is not observed on the HOPG surface, though the bulk crystalline phase on it is found similar to that on the Au(111) substrate. This indicates that the bulk molecular structure of the DNTT molecules solely depends on the surface texture of the substrate, while the electronic structure at the interface depends both on the surface texture and the interfacial behavior, which is quite interesting. Also, the observed molecular organization induced HOMO level splitting on the technologically relevant pc-Au surface, which has a tendency to reduce the hole injection barrier at the interface, has a strong implication on the charge transport properties of DNTT based devices.

## 2. Experimental details

The electronic structures of the DNTT molecular thin films on pc-Au and HOPG surfaces were characterized by photoelectron spectroscopic techniques in an ultrahigh vacuum (UHV) chamber (Omicron Nanotechnology, base pressure  $\sim 2.0 \times 10^{-9}$  mbar) [30]. The UHV chamber was equipped with an EA125 hemispherical energy analyzer along with two (UV and X-ray) light sources. A He gas discharge lamp (He I, of energy 21.2 eV) was used for UPS measurements, where the corresponding spectrometer energy resolution was  $\sim 0.1$  eV. All the UPS measurements were carried out applying a sample voltage of  $-6$  V to determine the higher binding energy cut-off (HBEC). UPS spectra were collected at a  $90^\circ$  take-off angle for higher photoelectron yield and all the spectra were collected at room temperature. For the XPS measurements, a monochromatic Al  $K_\alpha$  X-ray source (of energy 1486.6 eV) was used, where the corresponding spectrometer resolution was  $\sim 0.8$  eV.

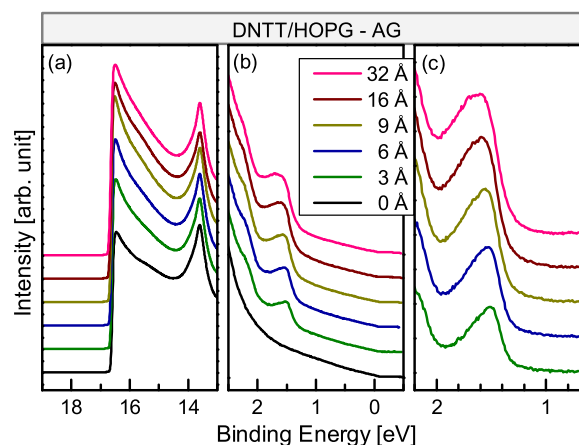


Fig. 1. UPS spectra of the as-grown (AG) DNTT/HOPG thin films of different cumulative nominal thickness ( $D_{CN}$ ) at the (a) HBEC region, (b) HOMO region and (c) substrate background-subtracted HOMO region.

pc-Au substrate, after inserting it into the UHV chamber, was cleaned by  $Ar^+$  ion sputtering and examined by XPS (as shown in Fig. S2 of the Supporting Information). The top layer of the HOPG substrate was peeled off, just before inserting it into the UHV chamber, to get a clean HOPG surface. A high-vacuum deposition chamber (base pressure  $\sim 1.0 \times 10^{-8}$  mbar) that is attached with the characterization chamber was used for thin film deposition. Thin films of DNTT (Sigma-Aldrich; purity: 99%) were deposited by thermal evaporation technique from a quartz crucible of a resistively heated Knudsen cell and keeping the substrates at room temperature. The deposition rate ( $\sim 1 \text{ \AA min}^{-1}$ ) was monitored by a quartz crystal microbalance (QCM). Thin films of cumulative nominal thickness ( $D_{CN}$ ) 3, 6, 9, 16, and 32  $\text{\AA}$  were deposited in steps on each substrate. Thin films of different nominal thicknesses were also deposited at a stretch for comparison. Annealing of the films after each step of deposition was performed at  $100^\circ\text{C}$  or  $120^\circ\text{C}$  for 1 h. In-situ UPS and XPS measurements were carried out for the DNTT thin films of different thickness, before and after annealing. Au  $4f_{7/2}$  level (binding energy of 84.0 eV) and C 1s level (binding energy of 284.4 eV for HOPG) were chosen as the reference levels for the films deposited on pc-Au (as shown in Fig. S3 of the Supporting Information) and HOPG substrates, respectively, to calibrate the other core level spectra [30]. The PeakFit software was used to analyze the XPS and UPS spectra. The Shirley method was used to subtract the XPS background, while the Gaussian–Lorentzian (GL) sum function was used to fit the XPS core-level spectra.

Topography of the deposited DNTT thick films, before and after AN, were studied ex-situ by an atomic force microscope (Nanoscope IV, Veeco) [31]. Topographic images of the DNTT films were collected using Al coated Si tip (radius of curvature  $\sim 10$  nm) in the tapping mode (drive frequency  $\sim 285$  kHz). WSXM software was used to process and analyze the AFM images [32].

## 3. Results and discussion

### 3.1. UPS study of the DNTT/HOPG films

The UPS spectra of the AG DNTT/HOPG thin films of different  $D_{CN}$ -value are shown in Fig. 1. In the HBEC region (Fig. 1(a)), a sharp peak at binding energy 13.6 eV is evident, which originates from the  $\sigma^*$  conduction band of the HOPG substrate [33]. The intensity of that peak decreases slightly with the increase of the film thickness, as expected. No appreciable shift in the vacuum level (VL), as obtained from the HBEC, is observed after deposition of the DNTT thin film of  $D_{CN}$ -value ranging from 3  $\text{\AA}$  (near monolayer [19,28]) to 32  $\text{\AA}$  (multilayer)

on HOPG substrate. This reflects near passive nature of the HOPG surface towards DNTT molecules and absence of any net molecular dipole moment in the thin film unlike polar phthalocyanine [30]. An asymmetric HOMO peak at  $\sim 1.5$  eV is observed for the 3 Å film, the position of which slightly shifts ( $\sim 0.1$  eV) towards higher binding energy side with the increase of the film thickness (see Fig. 1(b) and (c)). The asymmetric nature of the HOMO band possibly indicates the presence of unresolved fine structure, which originates from hole-vibration coupling, as observed previously in the pentacene/HOPG and rubrene/HOPG systems [34,35]. No increase in the intensity but a noticeable broadening of the HOMO band is observed with the increase of the film thickness, which can be attributed to the increase in the disorder.

The UPS spectra of the DNTT/HOPG thin films of different  $D_{\text{CN}}$ -value, annealed at 100°C after each step of deposition, are shown in Fig. 2. A sharp increase in the HOMO band intensity with a very small shift in the HOMO band position towards the higher binding energy side due to annealing, is observed. The maximum increase in the intensity due to annealing is mainly takes place for the 3 Å film. No further increase in the intensity due to annealing is observed for the thicker films rather a noticeable broadening of the HOMO band takes place. Same thing is also observed for the films of different thickness prepared at a stretch (as shown in Fig. S4 of the Supporting Information). In fact, the change (increase) in the HOMO band intensity of the thicker film (16 Å) after annealing is found to decrease compared to that of the thinner films. The broadening of the HOMO band with the increase of the film thickness is found appreciable for such AG films, while small but noticeable for the AN films. This result suggests that, in case of a 3 Å or near monolayer thick film, most of the molecules adsorb on the HOPG substrate in a flat-lying orientation to cover maximum surface area and to give rise an intense and sharp HOMO band. For further deposition, the molecules become gradually inclined or tilted in order to form bulk crystalline grains or domains with higher molecular packing, as observed before for the similar structured pentacene molecule on HOPG substrate [33,36]. The broadening of the HOMO band with increasing thickness can be attributed to the increase in the grain boundary related disorder. The large increase in the HOMO band intensity and decrease in the HOMO band width after annealing suggest that the molecules became more ordered in the monolayer region with flat-lying orientation and with greater coverage, and thereafter an increase in the grain size and decrease in the grain boundary related disorder. The hole injection barrier ( $\phi_{\text{BH}}$ ) at the DNTT/HOPG interface is found around 1.3 eV irrespective of film thickness and no significant change after annealing. The threshold IP is found around 5.8 eV, which is a little higher than that of the bulk value observed on Au surface [12]. The slight deviation in the IP of the DNTT/HOPG film is probably due to the different molecular organization, film morphology and/or interfacial behavior, where the formation of the interfacial dipole was not observed and the vacuum level alignment was governed by the non-interacting interface [33,37].

### 3.2. UPS study of the DNTT/Au films

The UPS spectra of the AG DNTT/Au thin films of different  $D_{\text{CN}}$ -value are shown in Fig. 3. The change in the VL, as evident from the HBEC region of the spectra (Fig. 3(a)), is found about  $-0.9$  eV for the 3 Å thick film, which increases to  $-1.1$  eV for the 32 Å thick film. These values are almost similar to those determined previously by Kelvin probe measurements [28]. The change of the VL is possibly due to the formation of interfacial dipoles caused by charge redistribution at the interface, generally observed after the adsorption of organic molecules on metallic surfaces. There are various mechanisms, like push-back effect, partial charge transfer, chemical interaction, or any permanent dipoles at the interface, which can be responsible for the formation of such interfacial dipole [30,38–40]. XPS technique can help to choose the possible mechanism, as discussed later. Here, the

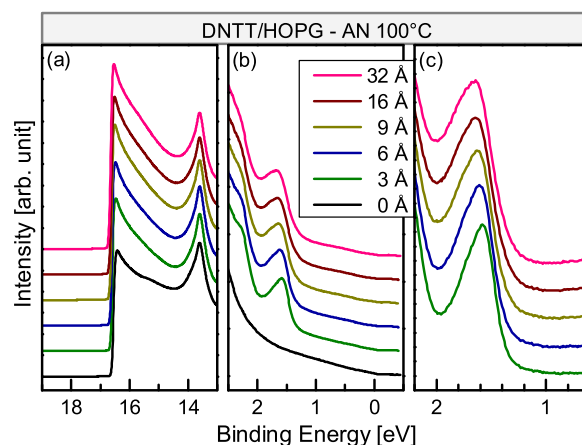


Fig. 2. UPS spectra of the DNTT/HOPG thin films of different cumulative nominal thicknesses annealed (AN) at 100°C (for 1 h after each step of deposition) at the (a) HBEC region, (b) HOMO region and (c) substrate background-subtracted HOMO region.

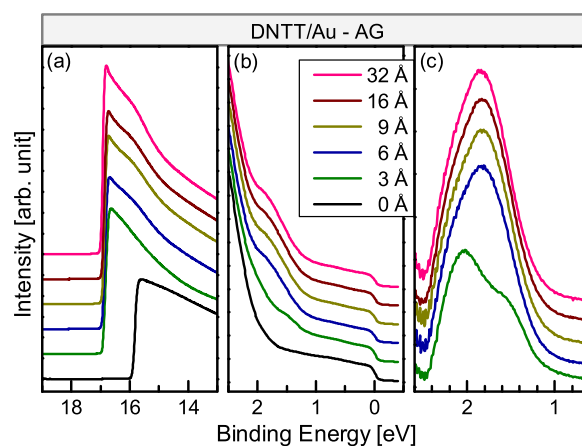


Fig. 3. UPS spectra of the as-grown (AG) DNTT/Au thin films of different cumulative nominal thicknesses at the (a) HBEC region, (b) HOMO region and (c) substrate background-subtracted HOMO region.

maximum change in the VL is observed for the 3 Å thick film and very small change thereafter. This result suggests that the interfacial dipoles are confined within the 3 Å film, possibly corresponding to the near monolayer structured DNTT molecules. Such monolayer confined interfacial dipoles indicate formation of a seed-layer at the interface that covers most of the pc-Au surface before further growth [40]. Formation of similar seed-layer of flat-lying molecules on pc-metal and dielectric substrates was observed before for DNTT and pentacene molecules [25,28,41]. No significant change in the VL is evident after annealing the film (see Fig. 4) suggesting no appreciable change in the seed-layer structure due to annealing.

A significant splitting in the HOMO level is observed for the 3 Å film, which almost disappear for the thicker films (see Fig. 3(b)). The HOMO level of the DNTT/Au film appears at the shoulder of the d-band of the Au substrate and thus it suppresses the intensity of the HOMO level. To overcome this the analysis was done for the substrate background-subtracted spectra as shown in Fig. 3(c). The energy difference between the split levels is found around 0.5 eV. Similar splitting of HOMO level was observed before in a densely packed monolayer phase but not in the loosely packed monolayer phase of the DNTT molecules on sc-Au(111) substrate [19]. The splitting of the HOMO level in the densely-packed monolayer phase on the DNTT/Au(111) system was attributed to the strong intermolecular interaction caused by substantial

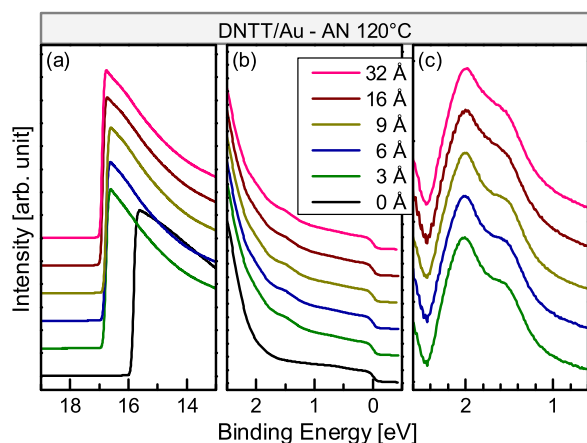


Fig. 4. UPS spectra of the DNTT/Au thin films of different cumulative nominal thicknesses annealed (AN) at 120°C (for 1 h after each step of deposition) at the (a) HBE region, (b) HOMO region and (c) substrate background-subtracted HOMO region.

overlapping of the molecular orbitals [19]. The structure of the similar-type pentacene molecules on the pc-Au surface was found different to that on the sc-Au(111) surface, irrespective of their surface roughness [41]. A seed-layer of flat-lying molecules in the monolayer region and crystalline domains with up-right oriented molecules in the subsequent region were found for the pentacene and DNTT molecules on the pc-Au surface [28,41]. Though a seed-layer of flat-lying molecules on the pc-Au surface was proposed, the splitting of HOMO level on the pc-Au surface, which is the signature of the strong intermolecular interaction of the seed-layer, has not been realized. The splitting of HOMO level in the 3 Å DNTT film on the pc-Au surface indicates the presence of seed-layer having strong intermolecular interaction, i.e., in the densely-packed phase. The formation of densely-packed monolayer phase having strong intermolecular interaction on both sc-Au(111) and pc-Au surfaces suggests that the material property and not the crystallographic structure of the substrate surface is important. Possibly, the interaction of the Au surface with the extended  $\pi$ -molecular orbital, though not very strong but sufficient enough to organize the molecules in a densely-packed monolayer structure, where most of the  $\pi$ -orbitals are in close contact with the Au surface. Due to this interaction, probably the pc-Au surface is also able to form a seed-layer of densely-packed phase, may be of partial coverage, before further growth.

The signature of this interaction is also evident in other step-deposited DNTT/Au films, after annealing them at 120°C, as shown in Fig. 4. The splitting feature of the HOMO level is clearly evident in different thick films, after annealing them at 120°C, though no change in the VL is observed. Such splitting is probably related to the conversion of different thick films to monolayer thickness due to the significant desorption of the molecules, placed above the monolayer, at 120°C. No splitting of HOMO level is observed in the films after annealing them at 100°C (as shown in Fig. S5 of the Supporting Information), suggesting no such conversion, probably due to the insignificant desorption of molecules at 100°C. Thus the HOMO level splitting phenomenon can be well attributed to the DNTT molecules present at the monolayer, which form more compact and stable structure compared to the molecules in the bulk film. This is further verified through XPS and AFM techniques as discussed later. The threshold IP for the AG 32 Å DNTT film is found around 5.4 eV, which is close to the reported value of the bulk DNTT film on Au surface. A slightly higher threshold IP (around 5.5 eV) is observed for the 3 Å film, while a slightly lower threshold IP (around 5.3 eV) is observed for the 32 Å film after annealing at 120°C. The  $\phi_{Bh}$  for the AG 32 Å DNTT film on the pc-Au surface is found around 1.2 eV, while that for the 3 Å DNTT film and other AN (at 120°C) DNTT films

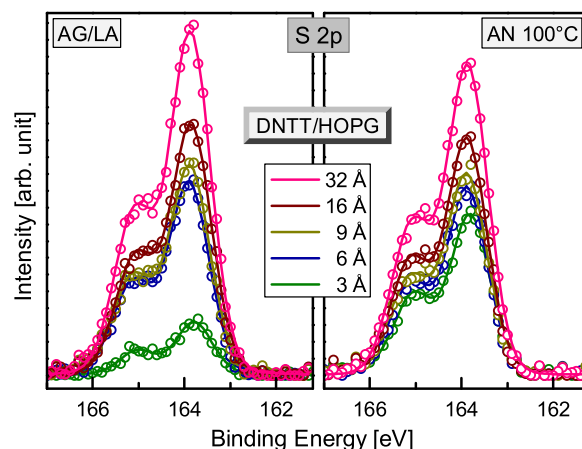


Fig. 5. S 2p core level spectra of the DNTT/HOPG thin films of different cumulative nominal thicknesses; (a) as-grown (AG/LA) on the substrate or on the last step deposited and annealed film and (b) annealed (AN) at 100°C for 1 h after each step of deposition.

on the pc-Au surface is found around 1.1 eV. A small decrease in the  $\phi_{Bh}$  value is probably related to the splitting nature of the HOMO level arising from the densely-packed monolayer phase on the pc-Au surface.

### 3.3. XPS study of DNTT/HOPG films

The S 2p core level spectra of the AG DNTT/HOPG thin films of different  $D_{CN}$ -value (as shown in Fig. S6 of the Supporting Information) suggest only an increase in the peak-intensity but no shift in the peak-position with the increase in the film thickness. An increase in the peak-intensity for the 3 Å film, after annealing it at 100°C, is clearly evident in Fig. 5. Similar phenomenon is also observed for the 6 Å film deposited at a stretch (shown in Fig. S7 of the Supporting Information). This increase is possibly due to an increase in the coverage of the DNTT film at the monolayer region as predicted from the increase in the HOMO level intensity. The increase in the peak-intensity for the 3 Å film, after annealing it at 120°C, is also observed (as shown in Fig. S8 of the Supporting Information). This result indicates reorganization of the DNTT molecules at the DNTT/HOPG interface due to thermal annealing, which leads to higher interfacial coverage of the flat-lying molecules. Not much decrease in the peak-intensity is observed for the films, having thickness higher than the monolayer thickness, even after annealing them at 120°C (as shown in Fig. S8 of the Supporting Information) suggesting not much molecular desorption. Probably the molecules above the interfacial layer are in the herringbone-like orientation to form better stable bulk crystalline phase as observed before on graphene surface [26], which restrict molecular desorption during annealing.

### 3.4. XPS study of the DNTT/Au films

The C 1s and S 2p core level spectra of the AG DNTT/Au thin films of different  $D_{CN}$ -value are shown in Fig. 6. The peaks corresponding to the C 1s and S 2p<sub>3/2</sub> core levels are found at  $284.8 \pm 0.1$  eV and  $164.1 \pm 0.1$  eV, respectively. No shift in the positions of the C 1s and S 2p core level spectra of the AG DNTT/Au thin films is observed with the increase of the film thickness indicating absence of any partial charge transfer or site-specific chemical interaction at the DNTT/Au interface [30,42]. The intensities of both the peaks are found to increase with the increase of the film thickness. However, the ratio of the two peaks, which is related to the ratio between C and S atoms, remains almost unchanged with the film thickness. The effect of annealing temperature on the C 1s core level spectra is shown in Figs. 7 and 8. No significant change in the peak-intensity is observed

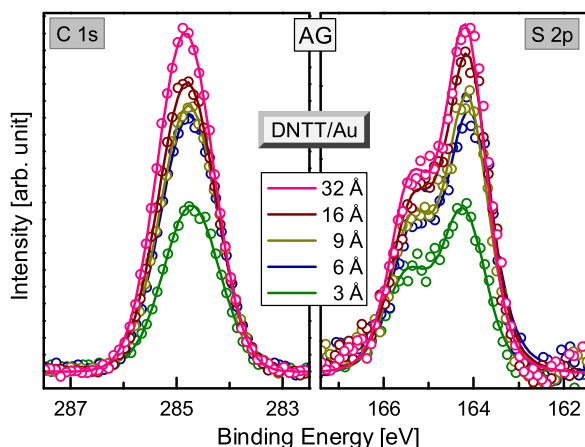


Fig. 6. C 1s and S 2p core level spectra of the as-grown (AG) DNTT/Au thin films of different cumulative nominal thicknesses.

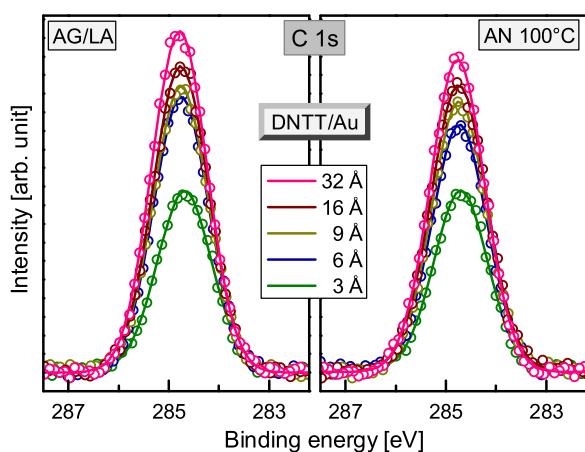


Fig. 7. C 1s core level spectra of the DNTT/Au thin films of different cumulative nominal thicknesses; (a) as-grown (AG/LA) on the substrate or on the last step deposited and annealed film and (b) annealed (AN) at 100°C for 1 h after each step of deposition.

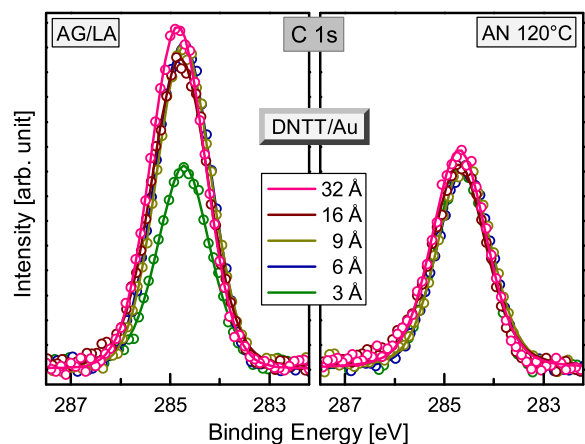


Fig. 8. C 1s core level spectra of the DNTT/Au thin films of different cumulative nominal thicknesses; (a) as-grown (AG/LA) on the substrate or on the last step deposited and annealed film and (b) annealed (AN) at 120°C for 1 h after each step of deposition.

for the 3 Å film, after annealing, while a significant decrease in the peak-intensity is observed for the films, having thickness higher than the monolayer thickness, after annealing them at 120°C (see Figs. 8). Such decrease is, however, negligible when annealed at 100°C (see

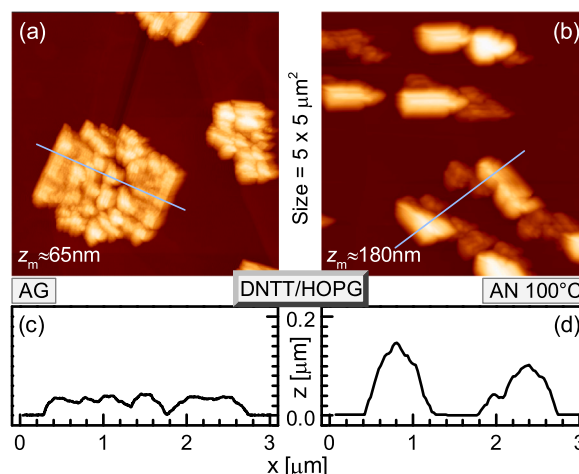
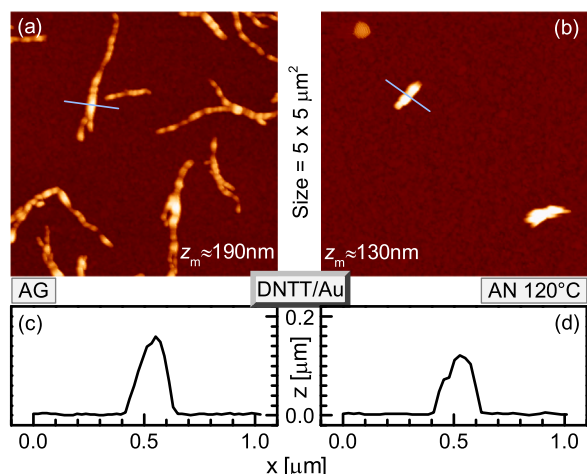


Fig. 9. AFM images (of scan size  $5 \times 5 \mu\text{m}^2$ ) of the (a) as-grown (AG) and (b) annealed (AN at 100°C) DNTT/HOPG thin film (of nominal thickness 32 Å).  $z_m$  indicates maximum height variation. (c) and (d) Height variations along the lines drawn through the respective images.

Fig. 7). It can be noted that though the peak intensity decreases in some cases with thermal annealing, but the ratio between C and S atoms remains almost unchanged, suggesting negligible dissociation of the molecules due to the thermal annealing. This also indicates significant desorption of the DNTT molecules during annealing the films at 120°C and negligible desorption when annealed at 100°C, verifying the inference made from the UPS result. It was reported earlier, from the thermal stability study of DNTT thin films on Ag(111) surface, that the molecular desorption is negligible below 112°C and the densely-packed interfacial molecules are thermally more stable than the other molecules [28]. Our results of DNTT films on the pc-Au surface are very much consistent with those results. The negligible molecular desorption in the 3 Å film indicates that the molecules at the interface are thermally more stable due to the densely-packed phase. The molecules at the interface possibly interact with the Au surface through the  $\pi$ -molecular orbitals resulting in better frontier  $\pi$ -orbital overlapping and thermal stability. The molecules above the interfacial layer are probably in the up-right orientation in order to form bulk crystalline phase as observed before for the similar types of molecular systems on polycrystalline surfaces [28,36] and hence are thermally less stable and desorb during annealing at 120°C.

### 3.5. AFM study of the DNTT/HOPG films

AFM images of the 32 Å DNTT/HOPG film, before (AG) and after annealing (AN) at 100°C, are shown in Fig. 9. Island-type growth of the film with partial coverage is evident from the topographic images (see Fig. 9(a) and (b)), which is due to the highly dewetting nature of the DNTT molecules on the HOPG surface as observed before [26]. With thermal annealing the height of the islands increases, while the size decreases as evident from the height profiles (Fig. 9(c) and (d)). Accordingly, the coverage of the islands decreases from about 20% for the AG film to about 13% for the AN film. Also each island, which was initially consists of a number of small molecular domains, coalesce after annealing to form a compact small island consisting of a single large molecular domain. This indicates that the annealing temperature provides the relaxation energy to the molecules to reorganize themselves to form larger crystalline domains and to reach the energy minimized bulk crystalline structure. Though the presence of separate interfacial layer can neither be confirmed nor be ruled out from the AFM images, the increase in the intensity of the HOMO level as well as the S 2p core level peak after thermal annealing can be



**Fig. 10.** AFM images (of scan size  $5 \times 5 \mu\text{m}^2$ ) of the (a) as-grown (AG) and (b) annealed (AN at  $120^\circ\text{C}$ ) DNTT/Au thin film (of nominal thickness  $32 \text{ \AA}$ ).  $z_m$  indicates maximum height variation. (c) and (d) Height variations along the lines drawn through the respective images.

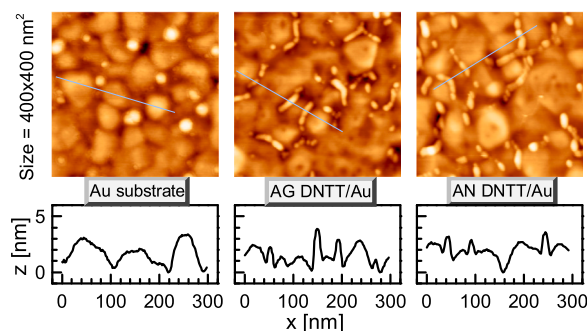


**Fig. 11.** AFM images (of scan size  $0.4 \times 0.4 \mu\text{m}^2$ ) of the Au substrate and the selected portion (where no large fiber-like structures are apparent in the large size scan) of the as-grown (AG) and annealed (AN at  $120^\circ\text{C}$ ) DNTT/Au thin film (of nominal thickness  $32 \text{ \AA}$ ), with typical height variations along the lines drawn through the respective images.

considered as the increase in the coverage and better organization of the flat-lying molecules in the wetted interfacial layer (similar to the pentacene molecules on HOPG [33]) and better organization of the molecules in the herringbone-like multilayer arrangement in the subsequent dewetted islands (similar to which was observed for the DNTT molecules on graphene [26]) to minimize the misfit related strain between two regions.

### 3.6. AFM study of the DNTT/Au films

AFM images of the  $32 \text{ \AA}$  DNTT/Au film, before (AG) and after annealing (AN) at  $120^\circ\text{C}$ , are shown in Fig. 10. Fiber-like structure with very low coverage (around 12%), which is a signature of highly dewetting nature of the DNTT molecules on the Au surface, is evident in the AG film (Fig. 10(a)). The average length, width and height of the fibers are found  $\sim 2.2 \mu\text{m}$ ,  $\sim 150 \text{ nm}$  and  $\sim 100 \text{ nm}$ , respectively. The coverage of such fiber-like structure became almost negligible after annealing the film at  $120^\circ\text{C}$  as shown in Fig. 10(b). This result supports well the UPS and XPS observations, namely significant molecular desorption of the DNTT/Au films (of thickness  $> 3 \text{ \AA}$ ) during annealing at  $120^\circ\text{C}$ .

AFM images for the selected portion of the  $32 \text{ \AA}$  DNTT/Au film, before (AG) and after annealing (AN) at  $120^\circ\text{C}$ , where no large fibers or apparent wetting of molecules were observed (in Fig. 10), are shown in Fig. 11. AFM image of the bare Au substrate is also included for comparison. Molecular wetting on that part is also evident. Small molecular

domains of low height, which is a clear signature of molecular wetting on the pc-Au substrate, even in the fiber free region, are observed. No molecular desorption from such interfacial domains is observed after annealing the film at  $120^\circ\text{C}$ . In fact, small increase in the number of these molecular domains is found after annealing. This result indicates that the packing and the structure of the molecules in these interfacial domains are different from those of the bulk-like domains. In fact, the presence of such thermally stable interfacial domains suggest the formation of the densely-packed herringbone-like seed-layer, similar to that observed for DNTT on sc-Au(111) [28], but with less coverage. While the desorption-prone subsequent fibers are likely to have up-right oriented structure, similar to that observed for DNTT on pc-Au surface [28]. Such dewetted fibers are formed above the thermally-stable partially-covered seed-layer to minimize the misfit related strain between two regions.

## 4. Overall picture and conclusions

Let us now first draw the energy-level diagrams (ELDs) and then model the configurations and organizations of the DNTT molecules on HOPG and pc-Au surfaces before and after annealing for different deposition amount to visualize the overall picture. The ELDs and the configurations of the DNTT molecules on the HOPG and pc-Au surfaces can be modeled using the information obtained from the complementary UPS, XPS and AFM techniques and the analogy found in the literature, as shown schematically in Fig. 12.

A highly-dewetting nature of the DNTT molecules above a relatively-wetted interfacial layer, i.e., Stranski–Krastanov-type growth mode, is observed on both the (HOPG and Au) substrates, probably to minimize the misfit related strain between two regions [28]. Island-type growth is observed for the multilayer thick DNTT film on HOPG substrate, where each island consists of a number of small molecular domains, which coalesce after annealing to form compact small-size islands consisting of a single molecular domain reducing the disorder. A fiber-like structural growth is observed for the multilayer thick DNTT film on pc-Au substrate, which desorbs at high temperatures ( $120^\circ\text{C}$ ) to retain the underlying densely-packed seed-monolayer. It would have been really interesting to estimate the critical thickness of the wetting layer and the molecular orientation in the island from the step height measured by the AFM. However, for that well resolved steps (in the order of monolayer or bilayer), which is probably possible using in-situ STM or AFM measurement facility, is necessary, as the presently measured steps are quite large and not sensitive for such estimation.

The formation of the interfacial dipole at the DNTT/Au interface, possibly due to the push-back (i.e., Pauli repulsion) effect [30,38–40], changes the VL of the pc-Au surface after deposition of the DNTT molecules. The change is about  $-0.9 \text{ eV}$  for the monolayer deposition, which becomes  $-1.1 \text{ eV}$  for thick multilayer deposition. The formation of seed-layer, in near monolayer thick film, seems to contribute in the major change of the VL. A significant HOMO level splitting (of amount  $\sim 0.5 \text{ eV}$ ) is observed for the monolayer thick film, which is, however, absent in other thick films. Such splitting of HOMO level indicates the presence of a strong intermolecular interaction arising from the frontier  $\pi$ -orbital overlapping in a densely-packed herringbone-like seed-layer on the pc-Au surface, similar to that observed on the sc-Au(111) surface [19,28], but probably with less coverage. Though, no site-specific chemical interaction or partial charge transfer is found in the system, it is likely that the Au surface still exerts some interaction towards the extended  $\pi$ -molecular orbital, which is sufficient enough to organize the molecules on the substrate surface in a densely-packed herringbone-like phase with partial coverage. Subsequent deposition forms fiber-like structure with up-right oriented molecules (i.e. in loosely packed bulk phase), desorption of which takes place easily due to the annealing at  $120^\circ\text{C}$  to retain the partially-covered highly-stable densely-packed herringbone-like seed-layer.

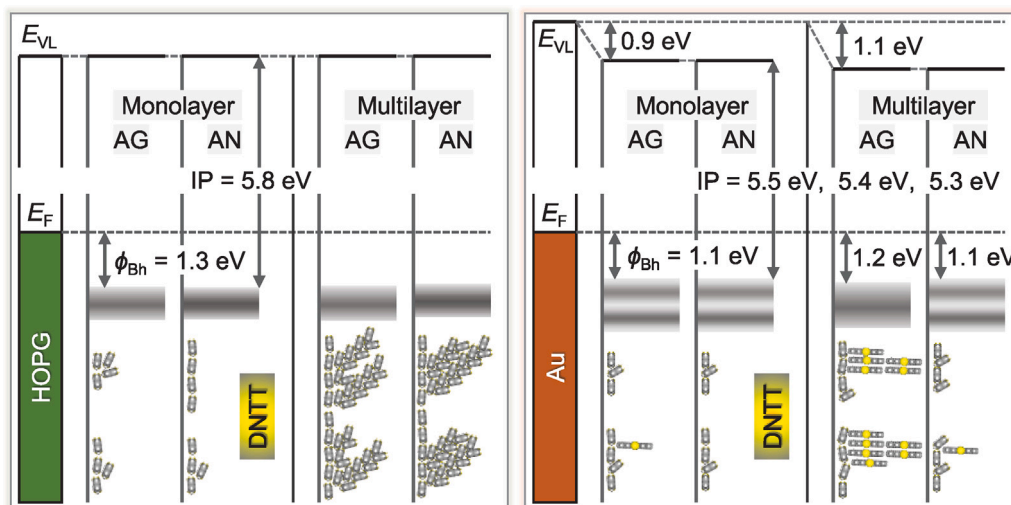


Fig. 12. Energy-level diagrams of DNTT/HOPG and DNTT/Au thin films of different nominal thicknesses before (AG) and after (AN) thermal annealing and their possible molecular configuration and organization at the interface and above, as predicted from UPS, XPS and AFM measurements.

It can be noted that on a clean Au(111) substrate, the DNTT molecules at first form an ordered monolayer with several rotational domains, where within each domain the aromatic rings are oriented parallel to the substrate surface, in a closely-packed (herringbone-like) manner, according to the van der Waals dimension of the molecules, as discussed before for DNTT [17,28] and pentacene (a similar type of molecule having similar adsorption geometry) [41] molecules. However, on the clean pc-Au surface, the molecules are unable to orient themselves in that closely-packed fashion due to the surface undulation, rather adsorb in flat-like face-on orientation to maximize the electronic interaction of the molecular  $\pi$ -system with the substrate, as discussed in many literature for this type of molecule. In subsequent layers the molecules follow face-on-like orientation but with little tilt compared to the molecules in the monolayer to form the preferred bulk crystalline phase with (12 $\bar{1}$ ) planes on Au(111). Consequently, there is a lattice mismatch between the interfacial layer and the subsequent layers, which resulted in a highly dewetted fiber-like structures, as discussed before [17,28]. However, this preferred bulk crystalline phase is not possible on the pc-Au surface due to the presence of rough or undulated seed layer. Hence the molecules follow other preferred crystalline phase, namely up-rightly oriented (001) structure.

The inactive nature of the HOPG surface [30] probably unable to form any interfacial dipole, which then fails to change its VL upon deposition of the DNTT molecules and also after subsequent thermal annealing. The molecules at the interface (for monolayer deposition) are near flat-lying to cover maximum surface area as observed for the pentacene molecules [33], which in the subsequent layers due to further deposition become inclined or tilted to form dewetted-islands with herringbone-like oriented molecules (i.e. in the crystalline bulk phase) [26]. That means the DNTT molecules initially adsorb in a flat-like orientation on the HOPG surface but not in a closely-packed manner that observed on the Au(111) substrate. Subsequently, the DNTT molecules on the HOPG surface (which is atomically flat in few micrometer range) follow the same structure like that on the Au(111) surface, namely the flat-like orientation but with little tilt to make (12 $\bar{1}$ ) planes of bulk crystalline structure, as the bulk crystalline structure with the fully flat-like molecules is not possible. This also causes a lattice mismatch at the interface resulting in a highly dewetted bulk structure. It can be noted that although the electronic structure and the interfacial molecular absorption or structure on HOPG (flat face-on oriented) and Au(111) (closely packed herringbone-like) are quite different but their bulk molecular structures are quite similar on both the surfaces, as the latter is mainly depends on the flat substrate surface and the ordered nature of the interfacial layer. Further, the ordering

of the molecules, both at the interface and in the islands, are found to increase considerably with the thermal annealing. The enhanced ordering of the molecules, particularly at the interface, plays important role to transform the as-grown weak and broad HOMO band to an intense and sharp HOMO band (as shown in Fig. 2).

The HOMO level splitting phenomenon of DNTT molecules was observed before on the Au(111) surface, but not on the pc-Au surface. In case of DNTT/Au(111) film, the molecules are adsorbed in a well-ordered monolayer phase but in multiple rotational domains. In each domain the molecules are closely-packed in a herringbone-like structure to overlap their molecular orbitals or to interact. But in case of DNTT/pc-Au, it was discussed [19,28] that since the substrate surface is not flat enough, it creates hindrance in the molecular adsorption to form similar closely-packed structure, rather the molecules on it adsorb in a flat-like orientation following the surface undulation. Accordingly, no intermolecular interaction due to the molecular orbital overlapping, which is solely depends on molecular packing and ordering, was expected. However, present study certainly indicates similar kind of interaction even on the pc-Au substrate (from the HOMO level splitting). This also indicates the presence of similar kind of domains (of closely packed molecules) at the DNTT/pc-Au interface, the size of which is certainly very small compared to that at the DNTT/Au(111) interface. The thermal stability of the molecules at the interfacial layer on pc-Au substrate also supports this result.

It can be noted that such interfacial layer on pc-Au substrate has not been observed before, which may be related to the relatively high roughness and/or lack-of Au(111) texture of the pc-Au substrate and also to the techniques used to observe. Though the observation of such structure directly through the complementary technique is demanding, the lack-of proper texture and high roughness of the pc-Au surface make it difficult to probe such structures even through the possible techniques like scanning tunneling microscopy (STM) or near edge X-ray absorption fine structure (NEXAFS). However, splitting of HOMO level for the monolayer thick DNTT film on the pc-Au surface certainly indicates the presence of a strong intermolecular interaction, which can only arise from the frontier  $\pi$ -orbital overlapping in a densely-packed herringbone-like seed-layer. As the pc-Au substrate is technologically more relevant and this splitting phenomenon has a tendency to reduce the hole injection barrier at the interface, so this result has a clear impact on the future device application on this type of molecules.

#### CRedit authorship contribution statement

**Subhankar Mandal:** Conceptualization, Methodology, Investigation, Data curation, Formal analysis, Writing – original draft. **Saugata**

**Roy:** Investigation. **Md Saifuddin:** Investigation. **Satyajit Hazra:** Conceptualization, Supervision, Visualization, Validation, Writing – review & editing.

### Declaration of competing interest

The authors declare that they have no known competing financial interests or personal relationships that could have appeared to influence the work reported in this paper.

### Acknowledgments

The authors thank Mr. G. Sarkar and Prof. M. Mukherjee for their technical support and fruitful discussion. S.M. acknowledges Council of Scientific & Industrial Research (CSIR), India and M.S. acknowledges University Grant Commission (UGC), India for providing research fellowships.

### Appendix A. Supplementary data

Supplementary material related to this article can be found online at <https://doi.org/10.1016/j.apsusc.2022.153696>.

### References

- [1] O. Ostroverkhova, Organic optoelectronic materials: Mechanisms and applications, *Chem. Rev.* 116 (2016) 13279–13412.
- [2] C.-H. Cheng, Z.-Q. Fan, S.-K. Yu, W.-H. Jiang, X. Wang, G.-T. Du, Y.-C. Chang, C.-Y. Ma, 1.1  $\mu\text{M}$  near-infrared electrophosphorescence from organic light-emitting diodes based on copper phthalocyanine, *Appl. Phys. Lett.* 88 (2006) 213505.
- [3] L. Xiao, Z. Chen, J. Qu, S. Kong, Q. Gong, J. Kido, Recent progresses on materials for electrophosphorescent organic light-emitting devices, *Adv. Mater.* 23 (2011) 926–952.
- [4] D.Y. Kim, F. So, Y. Gao, Aluminum phthalocyanine chloride/C60 organic photovoltaic cells with high open-circuit voltages, *Sol. Energy Mater. Sol. Cells* 93 (2009) 1688–1691.
- [5] A.W. Hains, Z. Liang, M.A. Woodhouse, B.A. Gregg, Molecular semiconductors in organic photovoltaic cells, *Chem. Rev.* 110 (2010) 6689–6735.
- [6] U. Zschieschang, F. Ante, T. Yamamoto, K. Takimiya, H. Kuwabara, M. Ikeda, T. Sekitani, T. Someya, K. Kern, H. Klauk, Flexible low-voltage organic transistors and circuits based on a high-mobility organic semiconductor with good air stability, *Adv. Mater.* 22 (2010) 982–985.
- [7] C. Wang, H. Dong, W. Hu, Y. Liu, D. Zhu, Semiconducting  $\pi$ -conjugated systems in field-effect transistors: A material odyssey of organic electronics, *Chem. Rev.* 112 (2012) 2208–2267.
- [8] O.A. Melville, B.H. Lessard, T.P. Bender, Phthalocyanine-based organic thin-film transistors: A review of recent advances, *ACS Appl. Mater. Interfaces* 7 (2015) 13105–13118.
- [9] Y. Huang, X. Gong, Y. Meng, Z. Wang, X. Chen, J. Li, D. Ji, Z. Wei, L. Li, W. Hu, Effectively modulating thermal activated charge transport in organic semiconductors by precise potential barrier engineering, *Nature Commun.* 12 (2021) 1–9.
- [10] M. Dreher, D. Kang, T. Breuer, G. Witte, Growth of extended DNNT fibers on metal substrates by suppression of step-induced nucleation, *Nanoscale Horiz.* 4 (2019) 1353–1360.
- [11] T. Yamamoto, K. Takimiya, Facile synthesis of highly  $\pi$ -extended heteroarenes, dnaphtho[2,3-b:2',3'-f]chalcogenopheno[3,2-b]chalcogenophenes, and their application to field-effect transistors, *J. Am. Chem. Soc.* 129 (2007) 2224–2225.
- [12] H. Yagi, T. Miyazaki, Y. Tokumoto, Y. Aoki, M. Zenki, T. Zaima, S. Okita, T. Yamamoto, E. Miyazaki, K. Takimiya, S. Hino, Ultraviolet photoelectron spectra of 2,7-diphenyl[1]benzothieno[3,2-b][1] benzothiophene and dinaphtho[2,3-b:2',3'-f]thieno[3,2-b]thiophene, *Chem. Phys. Lett.* 563 (2013) 55–57.
- [13] N. Sato, K. Seki, H. Inokuchi, Polarization energies of organic solids determined by ultraviolet photoelectron spectroscopy, *J. Chem. Soc., Faraday Trans. 2* 77 (1981) 1621–1633.
- [14] K. Kuribara, H. Wang, N. Uchiyama, K. Fukuda, T. Yokota, U. Zschieschang, C. Jaye, D. Fischer, H. Klauk, T. Yamamoto, K. Takimiya, M. Ikeda, H. Kuwabara, T. Sekitani, Y.-L. Loo, T. Someya, Organic transistors with high thermal stability for medical applications, *Nature Commun.* 3 (2012) 1–7.
- [15] S. Haas, Y. Takahashi, K. Takimiya, T. Hasegawa, High-performance dinaphtho-thieno-thiophene single crystal field-effect transistors, *Appl. Phys. Lett.* 95 (2009) 022111.
- [16] U. Zschieschang, F. Ante, D. Kälblein, T. Yamamoto, K. Takimiya, H. Kuwabara, M. Ikeda, T. Sekitani, T. Someya, J. Blochwitz-Nimoth, H. Klauk, Dinaphtho[2,3-b:2',3'-f]thieno[3,2-b]thiophene (DNNT) thin-film transistors with improved performance and stability, *Org. Electron.* 12 (2011) 1370–1375.
- [17] R. Takeuchi, S. Izawa, Y. Hasegawa, R. Tsuruta, T. Yamaguchi, M. Meissner, S. ichiro Ideta, K. Tanaka, S. Kera, M. Hiramoto, Y. Nakayama, Experimental observation of anisotropic valence band dispersion in dinaphtho[2,3-b:2',3'-f]thieno[3,2-b]thiophene (DNNT) single crystals, *J. Phys. Chem. C* 125 (2021) 2938–2943.
- [18] R.S. Sánchez-Carrera, S. Atahan, J. Schrier, A. Aspuru-Guzik, Theoretical characterization of the air-stable, high-mobility dinaphtho[2,3-b:2',3'-f]thieno[3,2-b]thiophene organic semiconductor, *J. Phys. Chem. C* 114 (2010) 2334–2340.
- [19] Y. Hasegawa, Y. Yamada, T. Hosokai, K.R. Koswattage, M. Yano, Y. Wakayama, M. Sasaki, Overlapping of frontier orbitals in well-defined dinaphtho[2,3-b:2',3'-f]thieno[3,2-b]thiophene and picene monolayers, *J. Phys. Chem. C* 120 (2016) 21536–21542.
- [20] Y. Zhang, J. Qiao, S. Gao, F. Hu, D. He, B. Wu, Z. Yang, B. Xu, Y. Li, Y. Shi, W. Ji, P. Wang, X. Wang, M. Xiao, H. Xu, J.-B. Xu, X. Wang, Probing carrier transport and structure–property relationship of highly ordered organic semiconductors at the two-dimensional limit, *Phys. Rev. Lett.* 116 (2016) 016602.
- [21] Q. Wang, S. Jiang, L. Qiu, J. Qian, L.K. Ono, M.R. Leyden, X. Wang, Y. Shi, Y. Zheng, Y. Qi, Y. Li, Interfacial flat-lying molecular monolayers for performance enhancement in organic field-effect transistors, *ACS Appl. Mater. Interfaces* 10 (2018) 22513–22519.
- [22] H. Chen, W. Zhang, M. Li, G. He, X. Guo, Interface engineering in organic field-effect transistors: Principles, applications, and perspectives, *Chem. Rev.* 120 (2020) 2879–2949.
- [23] M. Saifuddin, M. Mukhopadhyay, A. Biswas, L. Gigli, J.R. Plaisier, S. Hazra, Tuning the edge-on oriented ordering of solution-aged poly(3-hexylthiophene) thin films, *J. Mater. Chem. C* 8 (2020) 8804–8813.
- [24] M. Saifuddin, S. Roy, S. Mandal, S. Hazra, Vibronic states and edge-on oriented  $\pi$ -stacking in poly(3-alkylthiophene) thin films, *ACS Appl. Polym. Mater.* 4 (2022) 1377–1386.
- [25] M.-C. Jung, M.R. Leyden, G.O. Nikiforov, M.V. Lee, H.-K. Lee, T.J. Shin, K. Takimiya, Y. Qi, Flat-lying semiconductor–insulator interfacial layer in DNNT thin films, *ACS Appl. Mater. Interfaces* 7 (2015) 1833–1840.
- [26] T. Breuer, A. Karthäuser, H. Klemm, F. Genuzio, G. Peschel, A. Fuhrich, T. Schmidt, G. Witte, Exceptional dewetting of organic semiconductor films: The case of dinaphthothienothiophene (DNNT) at dielectric interfaces, *ACS Appl. Mater. Interfaces* 9 (2017) 8384–8392.
- [27] M. Geiger, R. Acharya, E. Reutter, T. Ferschke, U. Zschieschang, J. Weis, J. Pflaum, H. Klauk, R.T. Weitz, Effect of the degree of the gate–dielectric surface roughness on the performance of bottom-gate organic thin-film transistors, *Adv. Mater. Interfaces* 7 (2020) 1902145.
- [28] M. Dreher, D. Bischof, F. Widdascheck, A. Huttner, T. Breuer, G. Witte, Interface structure and evolution of dinaphthothienothiophene (DNNT) films on noble metal substrates, *Adv. Mater. Interfaces* 5 (2018) 1800920.
- [29] C. Zhang, H. Tsuboi, Y. Hasegawa, M. Iwasawa, M. Sasaki, Y. Wakayama, H. Ishii, Y. Yamada, Fabrication of highly oriented multilayer films of picene and DNNT on their bulklike monolayer, *ACS Omega* 4 (2019) 8669–8673.
- [30] S. Mandal, M. Mukherjee, S. Hazra, Evolution of electronic structures of polar phthalocyanine–substrate interfaces, *ACS Appl. Mater. Interfaces* 12 (2020) 45564–45573.
- [31] S. Roy, M. Saifuddin, S. Mandal, S. Hazra, Stearic acid mediated growth of edge-on oriented bilayer poly(3-hexylthiophene) Langmuir films, *J. Colloid Interface Sci.* 606 (2022) 1153–1163.
- [32] I. Horcas, R. Fernández, J.M. Gomez-Rodriguez, J. Colchero, J. Gómez-Herrero, A.M. Baro, WSM: A software for scanning probe microscopy and a tool for nanotechnology, *Rev. Sci. Instrum.* 78 (2007) 013705.
- [33] H. Fukagawa, H. Yamane, T. Kataoka, S. Kera, M. Nakamura, K. Kudo, N. Ueno, Origin of the highest occupied band position in pentacene films from ultraviolet photoelectron spectroscopy: Hole stabilization versus band dispersion, *Phys. Rev. B* 73 (2006) 245310.
- [34] H. Yamane, S. Nagamatsu, H. Fukagawa, S. Kera, R. Friedlein, K.K. Okudaira, N. Ueno, Hole–vibration coupling of the highest occupied state in pentacene thin films, *Phys. Rev. B* 72 (2005) 153412.
- [35] S. Duhm, Q. Xin, S. Hosoumi, H. Fukagawa, K. Sato, N. Ueno, S. Kera, Charge reorganization energy and small polaron binding energy of rubrene thin films by ultraviolet photoelectron spectroscopy, *Adv. Mater.* 24 (2012) 901–905.
- [36] H. Ozaki, Growth of organic ultrathin films studied by penning ionization electron and ultraviolet photoelectron spectroscopies: Pentacene, *J. Chem. Phys.* 113 (2000) 6361–6375.
- [37] I.G. Hill, A. Rajagopal, A. Kahn, Y. Hu, Molecular level alignment at organic semiconductor–metal interfaces, *Appl. Phys. Lett.* 73 (1998) 662–664.
- [38] H. Ishii, K. Sugiyama, E. Ito, K. Seki, Energy level alignment and interfacial electronic structures at organic/metal and organic/organic interfaces, *Adv. Mater.* 11 (1999) 605–625.
- [39] L. Wang, S. Chen, L. Liu, D. Qi, X. Gao, A.T.S. Wee, Thickness-dependent energy level alignment of rubrene adsorbed on Au(111), *Appl. Phys. Lett.* 90 (2007) 132121.

- [40] S. Sinha, M. Mukherjee, Thickness dependent electronic structure and morphology of rubrene thin films on metal, semiconductor, and dielectric substrates, *J. Appl. Phys.* 114 (2013) 083709.
- [41] D. Käfer, L. Ruppel, G. Witte, Growth of pentacene on clean and modified gold surfaces, *Phys. Rev. B* 75 (2007) 085309.
- [42] S. Sinha, M. Mukherjee, Study of metal specific interaction, F-LUMO and VL shift to understand interface of CuPc thin films and noble metal surfaces, *Appl. Surf. Sci.* 353 (2015) 540–547.